Thermal decomposition of HfCl$_4$ as a function of its hydration state

E. Barraud[a], S. Bégin-Colin[a,b,*], G. Le Caër[c], F. Villieras[d], O. Barres[d]

[a]*Laboratoire de Science et Génie des Matériaux et de Métallurgie, UMR CNRS INPL 7584, Ecole des Mines, F-54042 Nancy Cedex, France*
[b]*Institut de Physique et Chimie des Matériaux, GMI, UMR CNRS-ULP 7504, Ecole de Chimie, Polymères et Matériaux, 23,
rue du Loess, BP 43, F-67034 Strasbourg Cedex 2, France*
[c]*Groupe Matière Condensée et Matériaux, UMR CNRS-Université de Rennes-I 6626, Campus de Beaulieu, Bâtiment 11A, F-35042 Rennes Cedex, France*
[d]*Laboratoire Environnement et Minéralurgie, UMR CNRS-INPL 7569, Ecole Nationale Supérieure de Géologie de Nancy,
F-54501 Vandoeuvre-lès-Nancy Cedex, France*

Abstract

The thermogravimetric behavior of HfCl$_4$ powders with different hydration states has been compared. Strongly hydrated powders consist of HfOCl$_2 \cdot n$H$_2$O with $n > 4$. Partially hydrated powders consist of particles with a HfCl$_4$ core and a hydrated outerlayer of HfOCl$_2 \cdot n$H$_2$O with n in the range of 0–8. Hydrated powders decomposed at temperature lower than 200 °C whereas the decomposition of partially hydrated powders was completed at a temperature of around 450 °C. The observed differences in decomposition temperature is related to the structure of HfOCl$_2 \cdot n$H$_2$O, which is different if n is higher or smaller than 4 and leads to intermediate compounds, which decompose at different temperatures.

© 2006 Elsevier Inc. All rights reserved.

Keywords: Hafnium tetrachloride; Oxychloride octahydrate; Oxychloride; Hydration; Thermal decomposition; Structure

1. Introduction

MCl$_4$ compounds, with M = Zr, Hf, Ti, etc., are used as reactants in numerous solid–gas reactions to produce, for example, nitrides [1], in solid state or precipitation reactions to obtain carbides or borides [2–7] or with reductants to synthesize pure metals (Kroll process) [8] or oxides [9]. The properties of new ultra-high temperature ceramics, among which HfB$_2$ and MB$_2$/SiC (M = Zr and Hf), are currently being investigated with the aim of reaching high mechanical properties and oxidation resistance at temperatures higher than 1600 °C [10].

Metal chlorides are also involved in the synthesis of compounds with controlled shapes such as nanorods [1,4], hollow nanospheres [7] or in the atomic layer deposition process (ALD) [11–18]. The hydration reaction of HfCl$_4$, which is used to produce HfB$_2$ nanorods [4] or, which takes place during MO$_2$ or MB$_2$ (with M = Hf or Zr) ALD has been demonstrated to be an important, quite major, step [11,12,16,18,19]. In the ALD process, both the interaction of MCl$_4$ with hydroxyl groups at the surface of the Si substrate and with H$_2$O molecules and the control of the initial stage are of utmost importance for the resulting properties of the materials [11,12,16,18,19]. The yield of the synthesis reaction of HfB$_2$ nanorods, which consist in isothermal annealing of mechanically activated HfCl$_4$-based powder mixtures, and the formation mechanisms of these rods were also shown to be related to the hydration rate of HfCl$_4$ [4].

The characterization of the hydration of HfCl$_4$ and of its dehydration in various conditions is thus of interest for further controlling reactions involved in various synthesis methods such as reduction, ALD, etc.

Zirconium and hafnium chlorides are very hygroscopic. The hygroscopic behavior of all MX$_4$ tetrahalides (M = Ti, Zr, Hf and X = Cl, Br, I) is due to the strong affinity of the cation M^{4+} for O^{2-}. These compounds react spontaneously with liquid water and with water vapor to produce oxyhalides MOX$_2$ [20].

*Corresponding author. Institut de Physique et Chimie des Matériaux, GMI, UMR CNRS-ULP 7504, Ecole de Chimie, Polymères et Matériaux, 23, rue du Loess, BP 43, F-67034 Strasbourg Cedex 2, France. Fax: +33 3 88 10 72 47.

E-mail address: begin@ipcms.u-strasbg.fr (S. Bégin-Colin).

The violent and instantaneous hydrolysis of zirconium and hafnium tetrachlorides in water leads to the formation of an oxychloride octahydrate ($MOCl_2 \cdot 8H_2O$ with $M = Hf$ or Zr). Slower hydrolysis reactions may also occur by contact with wet air and leads to the formation of an hydrated oxychloride ($MOCl_2 \cdot nH_2O$) with an hydration rate n ranging between 0 and 8, depending on the temperature, the vapor pressure and the contact time [21–26]. Few studies were devoted to the intermediate products of hydration of $ZrCl_4$ or $HfCl_4$ [23–26]. Most studies dealt with $ZrOCl_2 \cdot 8H_2O$, aiming to characterize its structure and the polymerization conditions, which yield zirconia powders [27–36].

The aim of the present work is thus to characterize $HfCl_4$ powders with different hydration states by studying their dehydration by thermal annealing under argon. After having summarized literature results on the hydration products of Zr and Hf tetrachlorides and on their evolution during annealing in ambient air, we shall present and discuss our results on the dehydration of $HfCl_4$ powders with different hydration states during annealing in flowing argon and on their structure as a function of the hydration state.

2. Hydration products of hafnium and zirconium tetrachlorides

Only sparse investigations were devoted to chlorinated compounds of hafnium and to their transformations during annealing in various conditions [21–23]. In some cases, published results are available for the sole hydration products of $ZrCl_4$. They are nevertheless described below as they share common features with those of hafnium.

2.1. Hydration process

During the hydration of MCl_4 (with $M = Zr$ or Hf), the fixation of water molecules leads to hydroxichlorides of zirconium according to the hydrolysis reaction [23,26]:

$$MCl_4 + xH_2O \rightarrow M(OH)_xCl_{4-x} + xHCl \quad \text{with } x = 1 \text{ or } 2.$$
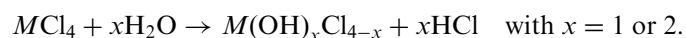
When the number of water molecules increases, the resulting hydrated hydroxichlorides $M(OH)_xCl_{4-x} \cdot yH_2O$ are unstable and transform into $MOCl_2 \cdot nH_2O$. $M(OH)_xCl_{4-x}$ was also reported to transform into $MOCl_2 + HCl$ and $MOCl_2 \cdot H_2O$ for $x = 1$ and 2, respectively.

Beden [23] modeled the hydration process of $ZrCl_4$ powders as schematized in Fig. 1. The volume change, which results from the hydration of $ZrCl_4$ leads to the cracking of the hydrated outer shells of particles, which become porous and favor the inward gaseous diffusion of water molecules and the outward gaseous diffusion of HCl molecules. Particles consist finally in $ZrCl_4$ cores surrounded by the latest formed zirconium oxychloride "subgrains" and by outer shell made of "sub-grains" with a
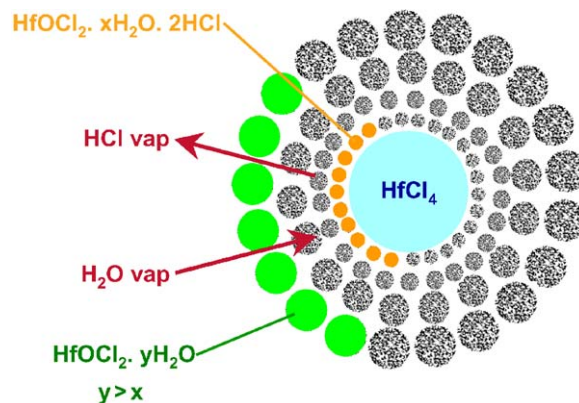

Fig. 1. Scheme of hydrolysis of an $HfCl_4$ particle [23].

composition close to that of a totally hydrated zirconium oxychloride. The hydration process of $HfCl_4$ is expected to be similar to that of $ZrCl_4$ (Fig. 1).

### 2.2. Structures of MCl_4 and of $MOCl_2 \cdot 8H_2O$

The structure of $ZrCl_4$ is monoclinic and has an AB_4-type structure (Fig. 2). It consists of a zig-zag chain of $ZrCl_6$ octahedrons (Fig. 2), coupled by two edges. The metal atoms form planar zig-zag chains; there are no Zr–Zr bonds in this chain [8,23,37–39].

The structure of hydroxy- or oxy-chlorides of hafnium- or zirconium-type compounds is complex because of a large variety of bonds (bridged or not) by ligands Cl$^-$, OH$^-$ and O^{2-} [40]. Clearfield and Vaughan [27] established that the structure of $ZrOCl_2 \cdot 8H_2O$, in solution and in crystalline solids [27,30,41] is based on a tetramer $[Zr_4(OH)_8(H_2O)_{16}]^{8+}$ associated with eight chloride ions in which Zr atoms form squares (Fig. 3). Every Zr atom shares a double OH bridge with each of its two Zr neighbors. Four water molecules are linked with every Zr atom and distort slightly the plane of the square [21,27–29,37,39] (Fig. 3). According to Beden [23], the structure of $ZrOCl_2 \cdot nH_2O$, with n in the range (0–8), depends on the hydration rate. From $n = 4$ up to a hydration rate of $n = 8$, the building block of the structure would be the tetrameric structure of $ZrOCl_2 \cdot 8H_2O$ as described by Clearfield and Vaughan [27]. For $n < 4$, the previous tetramer is replaced by a $Zr_a(OH)_b(H_2O)_c$ ($a \neq 4$) block with bridged Zr–O–Zr or Zr–OH–Zr bonds [23,42].

2.3. Decomposition during annealing in air

2.3.1. MCl_4 heat-treated in air ($M = Zr$ or Hf)

Annealing treatments of MCl_4 (with $M = Zr$ or Hf) in air (a slight hydrolysis occurs during heating) lead to the formation of MO_2 but the decomposition mechanisms are not truly understood. Different decomposition temperatures and mechanisms [23,25,36,43,44] were reported and are likely related to differences in the hydration states of the investigated MCl_4.
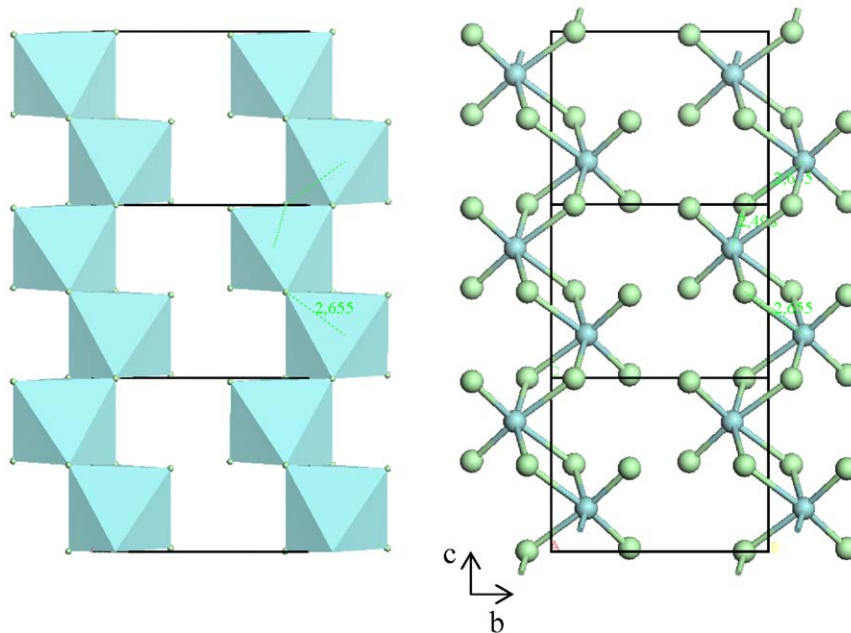
Fig. 2. Octahedral chains in ZrCl$_4$ [38].
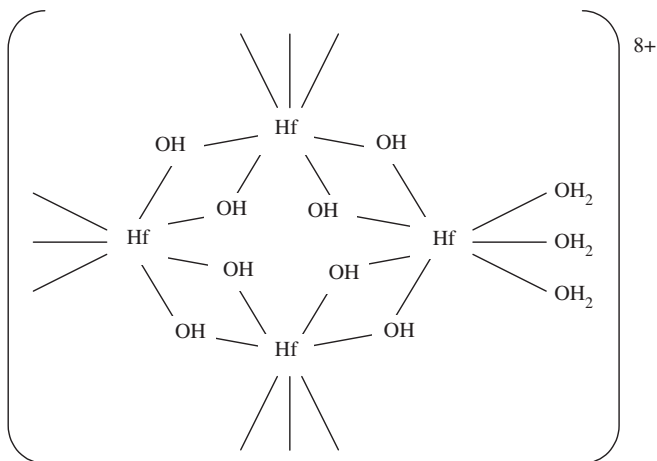
Fig. 3. Structure of $[Hf_4(OH)_8(H_2O)_{12}]^{8+}$ tetramer in HfOCl$_2 \cdot 4H_2O$ (proposed by Clearfield and Vaughan [27] for $[Zr_4(OH)_8(H_2O)_{12}]^{8+}$).

Benamira [43] reported a four-step thermal decomposition of HfCl$_4$ in air, which ends at about 450 °C. The successive steps consist in a dehydration of HfCl$_4$, a hydrolysis reaction, which results in the formation of HfOCl$_2$, a decomposition of HfOCl$_2$ to HfO$_2$ and a sublimation of HfCl$_4$ around 330 °C.

According to Beden [23] and Beden and Guillaume [25], ZrCl$_4$ would be transformed into ZrO$_2$ upon heating in air via the following reactions:

at $80-190\,^{\circ}\mathrm{C}$: $\mathrm{ZrCl_4 + 2H_2O \rightarrow Zr(OH)_2Cl_2 + 2HCl}$,

at $190-220\,^{\circ}\mathrm{C}$: $\mathrm{Zr(OH)_2Cl_2 \rightarrow ZrOCl_2 + H_2O}$,

at $220-325\,^{\circ}\mathrm{C}$: $\mathrm{2ZrOCl_2 + \frac{1}{2}O_2 \rightarrow Zr_2O_3Cl_2 + Cl_2}$,

at $325-750\,^{\circ}\mathrm{C}$: $\mathrm{Zr_2O_3Cl_2 + \frac{1}{2}O_2 \rightarrow 2ZrO_2 + Cl_2}$.
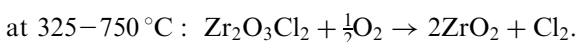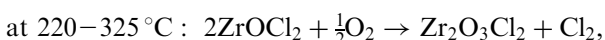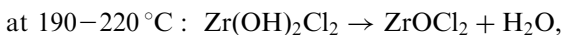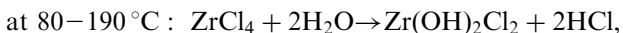
2.3.2. ZrOCl$_2 \cdot 8H_2O$

Most authors reported that ZrOCl$_2 \cdot 8H_2O$ first dehydrates down to $n = 4$ [23,31,36]. According to Komissarova et al. [31], after dehydration, the compound begins to decompose with a loss of chlorine at 80 °C, the decomposition being complete at 400–450 °C. Powers and Gray [36] reported that dehydration is complete at 700 °C. After Beden [23] and Beden and Guillaume [24], after dehydration ZrOCl$_2 \cdot 4H_2O$ is transformed successively into an amorphous Endemann chloride ZrO(OH)Cl $\cdot$ H$_2$O, then into Zr$_2$O$_3$Cl$_2 \cdot$ H$_2$O and finally into ZrO$_2$ around 150 °C. The latter temperature is consistent with the results of other studies on the thermal transformation of ZrOCl$_2 \cdot 8H_2O$, which report a temperature in the range 150–200 °C [21,45].

To summarize, there appears to be some confusion regarding the decomposition temperatures, which may be related to the uncertainties on the hydration states of the investigated compounds. Only a sparse number of papers have been devoted to the structures of hydrated HfCl$_4$ or ZrCl$_4$ and to their evolution with annealing treatments as a function of the hydration rate, especially for low hydration states [21–23,40]. Published results deal almost entirely with hydration products of ZrCl$_4$ and even if Hf-based compounds are generally thought to be isostructural with Zr-based compounds [23], it is necessary to investigate the specific case of HfCl$_4$ compounds due to their present and potential uses in the synthesis of various materials of engineering interest.

3. Experimental conditions

3.1. HfCl$_4$

Zirconium and hafnium are invariably associated in ores [21,22]. Zirconium and hafnium chlorides are obtained by

carbochlorination of zircon ores. Hafnium tetrachloride is usually separated from $ZrCl_4$ by extractive distillation [8,21,22]. The $HfCl_4$ compound studied in the present work results from such a process (Cezus Chimie, Jarrie, France) and was then stored in boxes closed under air. Its chemical analyzes showed that it is partially hydrated (Table 1). The water content was found to be about 1.6 wt%, from which it is found that the molecular composition is approximately $HfCl_4 \cdot 1/3H_2O$. However gaseous releases of HCl are detected when the boxes are opened, which means that water has soon interacted with $HfCl_4$. For brevity, this compound will be denoted hereafter as ph-$HfCl_4$, where ph stands for "partially hydrated".

The thermal behavior of ph-$HfCl_4$ powders was studied and compared to that of powders with different hydration states:

- a mainly anhydrous $HfCl_4$ powder obtained by storing $HfCl_4$ in argon directly after the extractive distillation step;
- two almost fully hydrated powders prepared either
  ○ by dissolving $HfCl_4$ into water at room temperature and then letting water evaporate in air (denoted as $HfCl_4$(water));
  ○ by exposing $HfCl_4$ powder to ambient air for 2 days (denoted as $HfCl_4$(air)).

3.2. Investigation techniques

Thermogravimetric analyzes (TGA) of powders were performed in flowing argon (99.9% pure, from Air Liquide) in a SETARAM B70 analyzer. Powders were heated at a rate of 5 °C/min up to 1100 °C, were then annealed at that temperature for 1 h and were finally cooled down to room temperature. The interpretation of the different steps (evaporation and/or decomposition of compounds) evidenced by TGA is based on characterizations performed by X-ray diffraction (XRD) and diffuse reflectance infrared Fourier transform (DRIFT) spectroscopy. XRD patterns were recorded with a Siemens D500 diffractometer using $CoK\alpha_1$ radiation ($\lambda = 0.17889$ nm). Infrared spectra were recorded with a Fourier transform infrared (FTIR) spectrometer (Bruker IFS 55) connected to a diffuse reflectance device (Harrick). Samples were gently ground and diluted in nonabsorbent KBr matrices (15 wt%). All spectra are recorded in flowing argon and shown in absorbance units.

4. Results

4.1. XRD characterization of powders

Fig. 4a shows the XRD pattern of ph-$HfCl_4$. The whole pattern consists of two superimposed patterns recorded in slightly overlapping high and low angle ranges, between 4° and 35° and between 20° and 110°, respectively. The very broad XRD peaks of starting ph-$HfCl_4$ cannot be indexed by the X-ray peaks of the sole $HfCl_4$ and are also attributed to $HfOCl_2 \cdot 6H_2O$. According to Beden [23], the XRD patterns of $ZrOCl_2 \cdot nH_2O$ are similar for different values of n. The data given in the JCPDS files of $HfOCl_2 \cdot nH_2O$ (Table 2) are indeed quite similar for $n = 6$ and 8, except for an additional peak at 8.6° for $HfOCl_2 \cdot 6H_2O$ and for the peak intensities (Table 2). However, according to its JCPDS file, the pattern of $HfOCl_2 \cdot 4H_2O$ differs more strongly from those given for $n = 8$ and 6, with, for example, no intense peak at around 8–9° (Table 2). The pattern of $HfOCl_2 \cdot 6H_2O$ matches quite well that of our ph-$HfCl_4$, especially in the 2θ range 24–34° (Fig. 4a).

However chemical analyzes (Table 1) reported indeed a composition of approximately $HfCl_4 \cdot 1/3H_2O$ for ph-$HfCl_4$. This is explained by the fact that XRD patterns were all recorded in air, as the very corrosive character of hydrochloric acid makes it difficult to use a protective environment to perform the X-ray analysis. Thus the XRD pattern of a ph-$HfCl_4$ sample differs likely from that of the stored ph-$HfCl_4$ (under argon) as hydration (due to the hygroscopic behavior of $HfCl_4$) occurs during XRD recording in air (30 min). For the same reason, the XRD pattern of anhydrous $HfCl_4$ powders is quite similar to that recorded with powders of ph-$HfCl_4$. Moreover the XRD pattern displays broad peaks, suggesting that the powders are quite amorphous and thus it is quite difficult to assign unambiguously the peaks.

The fully hydrated $HfCl_4$ powders have rather similar XRD patterns (Figs. 4b and c) and the X-ray peaks are also better indexed by the JCPDS peak positions of $HfOCl_2 \cdot 6H_2O$ than by those of $HfOCl_2 \cdot 8H_2O$. However, the XRD pattern of $HfCl_4$ (air) displays broader peaks than those of $HfCl_4$ (water) which may suggest that either the crystallites are very small or part of the sample is amorphous (Fig. 4b). By contrast, the narrow diffraction peaks of $HfCl_4$ (water) characterize a well-crystallized compound (Fig. 4c).

4.2. TGA experiments

The TGA curves of $HfCl_4$ powders with different hydration states are shown in Fig. 5.

4.2.1. Anhydrous HfCl₄

The TGA curve of anhydrous $HfCl_4$ displays a relative weight loss of about 95% (Fig. 5a). The final product is identified as HfO_2. Weight losses occur in two stages, with a very small loss between 100 and 200 °C and a very large
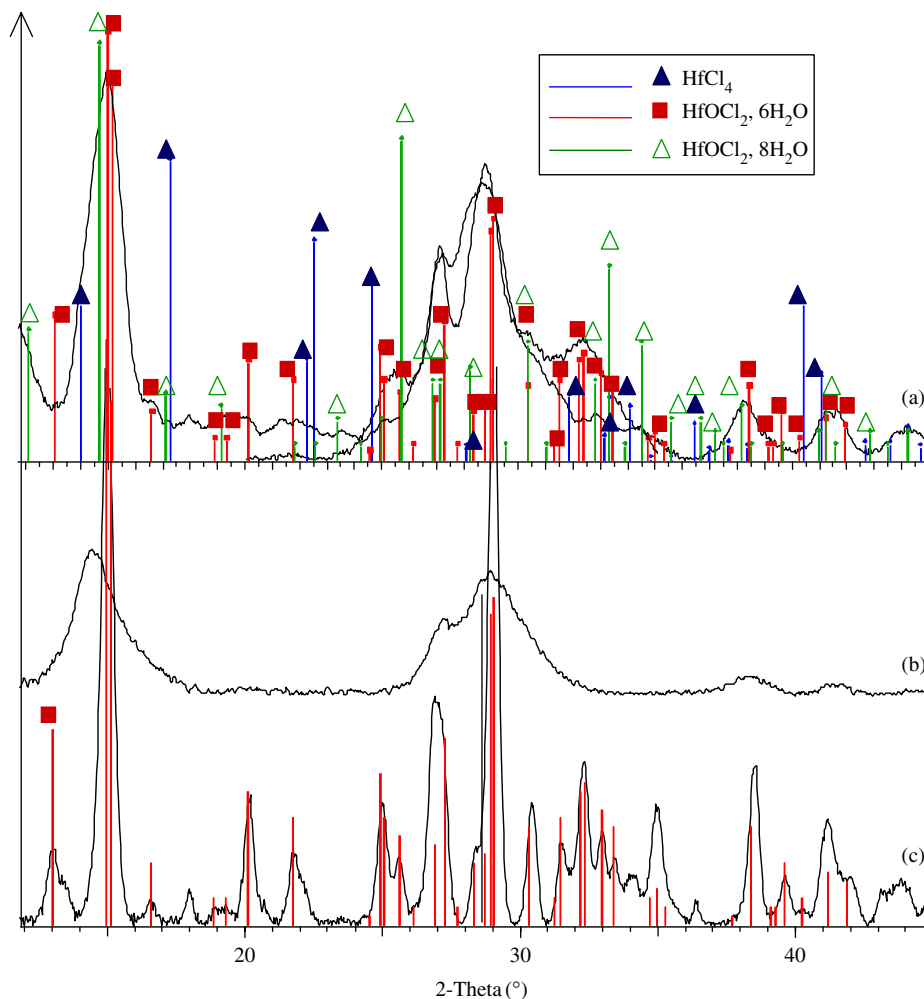
Table 1
Chemical composition of the ph-$HfCl_4$ (in brackets: contents expected for anhydrous $HfCl_4$)

Element	Hf	Cl	H	O
Composition (wt% ± 0.2)	54 (55.7)	44 (44)	1 (0)	1 (0)

Fig. 4. XRD pattern of: (a) ph-HfCl$_4$, (b) HfCl$_4$ (air) and (c) HfCl$_4$ (water).

loss between 200 and 300 °C. The latter stage is attributed to the sublimation of HfCl$_4$, which is known to occur at 317 °C at atmospheric pressure [46]. The presence of HfO$_2$ as a final residue shows that the starting anhydrous HfCl$_4$ is actually weakly hydrated. From the weight of HfO$_2$ residue after TGA (relative weight of about 5 wt%) and assuming the global reaction: HfCl$_4$ + 2H$_2$O → HfO$_2$ + 4HCl, simple calculations give an approximate composition of 6HfCl$_4 \cdot$ H$_2$O for the starting "anhydrous" HfCl$_4$.

Considering that the weight losses are only due to the sublimation of HfCl$_4$ and to an escape of hydrochloric acid HCl and thus neglecting the occurrence of a simultaneous dehydration reaction, we propose to describe the powder evolution according to:

$$HfCl_4 + \tfrac{1}{6}H_2O \rightarrow \tfrac{1}{6}Hf(OH)Cl_3 + \tfrac{5}{6}HfCl_4 + \tfrac{1}{6}HCl. \qquad (1)$$
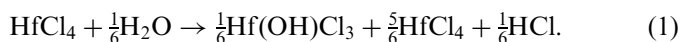
Then Hf(OH)Cl$_3$ would decompose according to two reactions:

$$Hf(OH)Cl_3 \rightarrow HfOCl_2 + HCl, \qquad (2)$$

$$2HfOCl_2 \rightarrow HfO_2 + HfCl_4. \qquad (3)$$
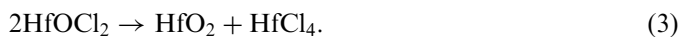
The expected weight loss due to the formation of HCl, 3.7 wt% (Eqs. (1) and (2)), agrees with the measured loss, around 3.5 wt%, measured on the TGA curve below 200 °C (Fig. 5a). The decomposition of anhydrous HfOCl$_2$ (Eq. (3)) and the subsequent formation of HfO$_2$ may occur at temperatures around or higher than 200 °C.

The total weight loss (Fig. 5a) is finally that obtained from the global reaction:

$$HfCl_4 + \tfrac{1}{6}H_2O \rightarrow \tfrac{1}{12}HfO_2 + \tfrac{11}{12}HfCl_4 + \tfrac{1}{3}HCl,$$

in agreement with experiment.

4.2.2. Strongly hydrated HfCl$_4$

HfCl$_4$ (air) and HfCl$_4$ (water) (Figs. 5b and c, respectively) show similar TGA curves displaying a regular weight loss from room temperature up to 160 and 200 °C, respectively. The final product in all cases is HfO$_2$.

From the weight of residual HfO$_2$ (relative weight of about 55 wt%) and considering the following global

reaction of formation of hafnia from $HfOCl_2 \cdot nH_2O$:

$$HfOCl_2 + nH_2O \rightarrow HfO_2 + 2HCl + (n-1)H_2O,$$

Table 2
JCPDS files of $HfOCl_2 \cdot nH_2O$ with $n = 4, 6$ and 8

$HfOCl_2 \cdot 8H_2O$ JCPDS no. 15-0348		$HfOCl_2 \cdot 6H_2O$ JCPDS file no. 47-0816		$HfOCl_2 \cdot 4H_2O$ JCPDS file no. 15-0380	
2θ	Intensity	2θ	Intensity	2θ	Intensity
8.479	100	8.247	100		
		9.992	44	10.162	90
12.067	20	12.968	22	11.940	20
14.620	65	14.918	66		
		15.089	59	15.578	100
17.061	10	16.522	7		
19.105	8	18.830	3		
		19.293	3		
21.755	2	20.071	15	20.822	40
22.575	2	21.734	12		
23.351	6	24.507	1		
24.184	2	24.898	17	24.127	60
24.968	6	25.038	12		
25.667	50	25.600	10		
		26.113	2		
26.834	12	26.894	9		
27.099	12	27.242	21	27.525	70
28.166	14	28.317	7		
		28.725	8	28.611	80
29.511	2	28.936	35		
		29.039	37		
30.342	18	30.315	11		
31.030	2	31.252	3	30.785	50
		31.469	12		
		32.181	15		
		32.348	16		
32.801	12	32.967	13	33.542	30
33.320	30	33.421	11		
33.902	2	34.726	3	34.224	35
34.493	18	34.961	4		
35.601	6	35.277	2		

the number of water molecules associated with $HfOCl_2$ is calculated to be 7.5 for $HfCl_4$ (water) and 5.5 for $HfCl_4$ (air). As expected, n is larger for the former compound than for the latter. The hydration rate found for $HfCl_4$ (air), $HfOCl_2 \cdot 5.5H_2O$, is consistent with the previous indexation of its XRD pattern with the JCPDS file of $HfOCl_2 \cdot 6H_2O$. However the pattern given by the latter file agrees better with that of $HfCl_4$ (water) (end of Section 4.1). Despite their limited dependences on n ($n \geqslant 6$), the question of the real values of the hydration states given in the JCPDS files of the $HfOCl_2 \cdot nH_2O$ compounds is raised.

TGA curves show no feature above 200 °C, these hydrated oxychlorides are totally transformed below 200 °C. The difference, ≈ 40 °C, between the final decomposition temperatures of these two compounds (Figs. 5b and c) is explained by the difference in their hydration states and in their crystallization states.

4.2.3. Partially hydrated "ph-HfCl₄"

The final product of the thermal decomposition of ph-$HfCl_4$ consists of monoclinic hafnia. Four features are observed on the TGA curve (Fig. 5d), two of them displaying significant weight-loss rates. The comparison with the TGA curves of strongly hydrated and anhydrous powders (Fig. 5) shows that the thermal decomposition of ph-$HfCl_4$ is a more complicated process. Sublimation of $HfCl_4$ occurs from 240 to 300 °C as observed for anhydrous $HfCl_4$ as well as a small weight loss at temperature below 200 °C. Such a weight loss just below 200 °C was also observed for $HfCl_4$ (air) and $HfCl_4$ (water) and was attributed to decomposition of $HfOCl_2 \cdot nH_2O$, for which $n \geqslant 4$. Weight losses take place also at higher temperatures than those found from the other TGA curves. Thus we may advance that ph-$HfCl_4$ powders contain $HfCl_4$, $HfOCl_2 \cdot nH_2O$ with $n \geqslant 4$ and further other compounds, which decompose at higher temperatures.
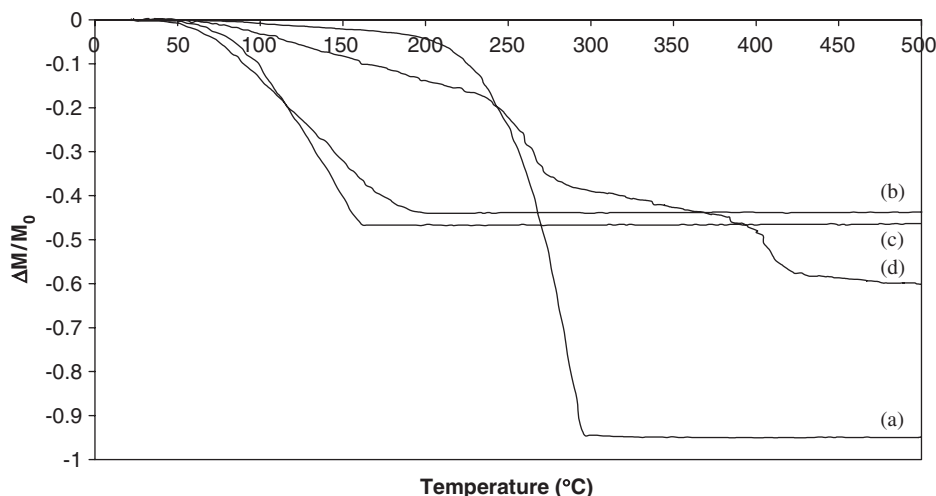

Fig. 5. TGA curves of $HfCl_4$ for different hydration states: (a) anhydrous $HfCl_4$, (b) $HfCl_4$ (air), (c) $HfCl_4$ (water), and (d) ph-$HfCl_4$.

Beden [23] concluded that partially hydrated $ZrCl_4$ ($ZrOCl_2 \cdot nH_2O$ with $n < 4$) decompose under air just below 700 °C while strongly hydrated $ZrCl_4$ ($n \geqslant 4$) decompose below 150 °C. Transposing Beden's results to hafnium compounds, the high temperature features may be attributed to the decomposition of $HfOCl_2 \cdot nH_2O$ with $n < 4$. The model of hydration of $ZrCl_4$ powders proposed by Beden [23] and sketched in Fig. 1 may as well explain the presence of all these phases in ph-$HfCl_4$. ph-$HfCl_4$ powders are thus composed of particles with a $HfCl_4$ core and an outer layer of $HfOCl_2 \cdot nH_2O$ with an hydration gradient.

To better identify the origins of the weight losses evidenced by TGA for ph-$HfCl_4$, the powders have been characterized by FTIR spectroscopy.

4.3. Infrared spectroscopy on ph-HfCl$_4$ powders

IR spectra of the starting ph-$HfCl_4$ and of those of the same powder heated at three temperatures selected from the TGA curve are given in Fig. 6.

At room temperature and under atmospheric pressure, the IR spectrum corresponds to that generally displayed for a hydrated hafnium oxychloride [23,36,42,47]. The broad vibration band between 3650 and 2600 cm^{-1} is associated with the OH stretching of water molecules (physisorbed molecular water) while those at 1616 cm^{-1} are associated with their bending mode (Table 3). The position of this band at 1616 cm^{-1} instead of 1630 cm^{-1}, which is usually found, confirms that the water molecules are coordinated to cations as in the tetramer structure of $ZrOCl_2 \cdot 8H_2O$.

The band at 2350 cm^{-1} is attributed to harmonic and/or to combination of vibration band of water and those at 2070 and 1830 cm^{-1} to bands of Hf–OH (Table 3).

A shoulder is observed at around 3700 cm^{-1}. Bands at wavenumbers higher than 3600 cm^{-1} are generally attributed to OH in Zr–OH (free) groups (terminal or bridged) [18,48,49].

The vibration bands at 1025, 930 and 720 cm^{-1} would originate from Hf–OH bonds (Table 3). More precisely, Powers and Gray [36] assigned the band at 1025 cm^{-1} to the bridging hydroxide deformation in association with a band at higher wavenumber around 3700 cm^{-1} and proposed that bands at 945 and 914 cm^{-1} and around 700–800 cm^{-1} could be associated with modes of coordinated water.

At 230 °C (Fig. 6b) the intensities of the vibration bands of water have strongly decreased, showing that hydration water molecules have disappeared. The broad band initially between 3650 and 2600 cm^{-1} is now located at about 3430 cm^{-1} and is characteristic of more free OH groups of Hf–OH type. The vibration bands between 1030 and 700 cm^{-1} attributed to Hf–OH bonds have disappeared.

The spectra recorded at 230, 320 and 420 °C (Figs. 6b–d) are similar in shape except that intensities of water bands decrease when the temperature increases. At 420 °C, a peak characteristic of monoclinic hafnia appears clearly at 754 cm^{-1} [22,42,47].

The IR results first show that Hf-based compounds with Hf–OH bonds are identified in ph-$HfCl_4$ powders. They decompose on heating below 230 °C. These OH bonds confirm that $HfOCl_2 \cdot nH_2O$ compounds with $n \geqslant 4$ and a tetrameric structure are present in the ph-$HfCl_4$ powders
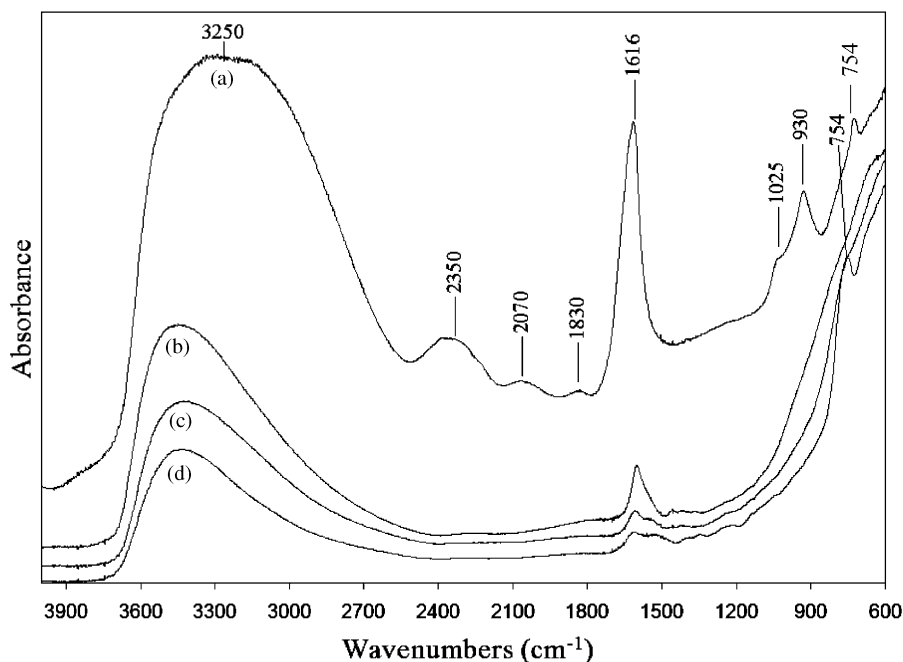

Fig. 6. FTIR spectra of ph-$HfCl_4$ in flowing argon at: (a) room temperature, (b) 230 °C, (c) 320 °C and (d) 420 °C (samples are heated under flowing argon at the given temperature for 90 min and analyzed after cooling down to room temperature).

Table 3
Infrared results of ph-HfCl$_4$ powders

Assignment	ph-HfCl$_4$ (cm^{-1})	ph-HfCl$_4$ heat-treated at 230 °C (cm^{-1})	ph-HfCl$_4$ heat-treated at 420 °C (cm^{-1})
OH stretching in Zr–OH free groups	Shoulder at 3700		
OH stretching of water molecules	Broad band centred at around 3250	Broad band centred at 3430 lower intensity (l.i.)	Broad band centred at 3430 lower intensity (l.i.)
Harmonic and/or combination of vibration bands of water	2350		
Harmonic and/or combination of vibration bands of Hf–OH	2070, 1830		
Bending mode of water molecules coordinated to cations	1616	1603 l.i.	1612 l.i. 1530
Hf–OH bonds:bridging hydroxide deformation [36]	1025		
Modes of coordinated water [36]	930, 720		
Monoclinic hafnia			754

and that they disappear below 230 °C. The IR results then show that HfO$_2$ is identified at temperatures higher than 320 °C. Between 320 and 420 °C, the main observations are the disappearance of bands associated with water and the crystallization of hafnia. The weight loss observed around 400 °C may thus be attributed to dehydration or dehydroxylation and crystallization of hafnia as observed by Guo and Chen [50] and by Pan et al. [51] during thermal treatment of zirconium hydroxide xerogels.

5. Mechanisms of thermal decomposition

5.1. Anhydrous HfCl$_4$

The TGA curve of anhydrous HfCl$_4$ shows that this powder is actually weakly hydrated with a composition HfCl$_4 \cdot 1/6$H$_2$O. Following Beden [23], the proposed mechanism is, for a composition near HfCl$_4$, the formation of a Hf(OH)Cl$_3$ compound by reaction on heating between HfCl$_4$ and H$_2$O. It further decomposes in HfOCl$_2 \cdot$. Then the latter compound transforms in HfO$_2$ at a temperature lower than 290 °C. The formation of an intermediate Hf(OH)Cl$_3$-type compound, before HfOCl$_2$, would agree with a substitution reaction of Cl by OH from water on heating.

5.2. Hydrated powders: HfOCl$_2 \cdot n$H$_2$O with $n \geqslant 4$

XRD patterns of strongly hydrated powders (HfCl$_4$ (air) and (water)) demonstrate that powders consist in HfOCl$_2 \cdot n$H$_2$O with $n > 5$. TGA experiments show that they decompose at temperatures below 200 °C. This result is consistent with the decomposition temperature, between 150 and 200 °C, reported for ZrOCl$_2 \cdot 6$H$_2$O [21,23,45]. The higher reported decomposition temperatures (see Section 2) above 250 °C may be attributed to the fact that the hydration rate of the investigated compounds was lower than expected [31,36].

The basic structural element of HfOCl$_2 \cdot n$H$_2$O with $n \geqslant 4$ is a tetramer presented in Fig. 3. After Beden [23], upon

heating the reaction of Cl$^-$ and OH$^-$ with Hf atoms from the tetramer leads to the formation of Hf$_2$O$_3$Cl$_2 \cdot 3$H$_2$O (or Hf$_2$(OH)$_6$Cl$_2$), which gives in turn Hf$_2$O$_3$Cl$_2 \cdot$H$_2$O (or Hf$_2$O$_2$(OH)$_2$Cl$_2$), which leads finally to the formation of HfO$_2$ and to a loss of HCl. However in studies conducted with ZrOCl$_2 \cdot 8$H$_2$O, when zirconia is synthesized by precipitation and calcination, no chlorination of zirconium occurs, the precipitate is an amorphous hydrous ZrO$_2$ obtained by an hydrolytic polymerization [30]. The polymerization of tetrameric ions takes place by formation of double hydroxyl bridges between tetrameric units (Zr(OH)$_4$, xH$_2$O) (e.g. olation between tetramer groups) [28–30,32].

Considering the tetramer structure (Fig. 3), upon heating, dehydration occurs and chlorine ions may react with released water to form HCl or to chlorinate Hf cations. In the latter case, an intermediate compound is based on Hf atoms linked by double bridged OH and with hydroxyl and chlorine groups. This corresponds to the scheme proposed by Beden and would lead to the formation of an Hf$_2$O$_2$(OH)$_2$Cl$_2$-type compound by condensation reactions of bridged OH. If no chlorination of hafnium ions occurs, the last product before HfO$_2$ would be a hydroxide. However, decompositions of hydroxides occur at temperatures higher than those observed here [30,41,50,51]. The most probable mechanism of decomposition of HfOCl$_2 \cdot n$H$_2$O with $n \geqslant 4$ appears thus to be that proposed by Beden [23], which does not involve hydroxides as intermediate compounds.

5.3. ph-HfCl$_4$

From previous results, we have shown that ph-HfCl$_4$ powders consist in particles with a HfCl$_4$ core and a hydrated outer layer of HfOCl$_2 \cdot n$H$_2$O with $0 \leqslant n \leqslant 8$. The low-temperature features in TGA curve are thus mainly due to the decomposition of HfOCl$_2 \cdot n$H$_2$O with $n \geqslant 4$ while the high-temperature ones ($T \geqslant 300$ °C) are attributed to the decomposition of HfOCl$_2 \cdot n$H$_2$O with $n < 4$.

The decomposition mechanisms proposed for $HfOCl_2 \cdot nH_2O$ with $n \geqslant 4$ cannot be applied to compounds with $n < 4$ as their structure is not built from a tetramer (Fig. 3). Considering that the structure of $HfCl_4$ is built from chains of $HfCl_6$ octahedra (Fig. 2), the Cl atoms, which may first be substituted by OH, are those, which are not involved in bridged bonds. Two chlorine atoms linked with each Hf atom may be thus substituted. Considering the chain structure of $HfCl_4$ and the resulting positions of Hf–OH bonds (Fig. 7), Hf–O–Hf bonds may form by a condensation mechanism with a release of water, leading to $HfOCl_2$, according to the following reaction scheme:

$$HfCl_4 + 2H_2O \rightarrow Hf(OH)_2Cl_2 + 2HCl \rightarrow HfOCl_2 + H_2O.$$
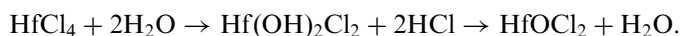
Water may also further be coordinatively bound to Hf atoms to form $HfOCl_2 \cdot nH_2O$ with $n < 4$. In these compounds, Hf atoms are connected to their Hf neighbors through Hf–O–Hf bonds and by double bridged Cl bonds in contrast to $HfOCl_2 \cdot nH_2O$ with $n \geqslant 4$, which displays only double bridged OH bonds. This difference in structure may explain the different thermal decomposition behavior as a function of the hydration rate.

Upon heating, $HfOCl_2$ is probably further hydrolyzed to yield hafnium hydroxides. This is consistent with IR spectra of powders heat-treated at $320\,^\circ C$ where hydroxides (Hf–OH) are identified. This scheme is also consistent with the weight losses observed at high temperature. Indeed Guo et al. [41] and Guo and Chen [50] observed a weight loss around $460\,^\circ C$ on the TGA curve of zirconium hydroxide obtained at pH = 4. They attributed it to a rapid release of bound hydroxyl groups resulting in the fast crystallization of zirconia. We may thus advance that during heating, $HfOCl_2 \cdot nH_2O$ with $n < 4$ transforms in an hafnium hydroxide, which transforms in turn at around $420\,^\circ C$ in HfO_2. Guo et al. [41] and Guo and Chen [50] pointed out that the weight loss at this temperature is observed only with an hydroxide whose structure differs from those of the known zirconium hydroxides. The structure proposed by Guo and Chen [50] is $Zr_2O_3(OH)_2 \cdot H_2O$, with Zr–O–Zr bonds, one monolinked OH per Zr and a water molecule coordinatively bound. This structure may be obtained from the above proposed mechanism for $HfOCl_2 \cdot nH_2O$ with $n < 4$ by hydrolysis of Cl double bridged bonds and then condensation reactions.

6. Conclusion

The thermal behaviors of $HfCl_4$ powders with different hydration states were compared. Weakly hydrated powders decompose by $HfCl_4$ sublimation and yield a small residual fraction of hafnia. Hydrated powders consist in $HfOCl_2 \cdot nH_2O$ with $n \geqslant 4$ and with a tetrameric structure and decompose at temperature below $200\,^\circ C$.

The partially hydrated powders (ph-$HfCl_4$) consist in particles with a $HfCl_4$ core and a hydrated outer layer of $HfOCl_2 \cdot nH_2O$ with $0 \leqslant n \leqslant 8$. Several features are observed on the TGA curve. Beyond the sublimation of anhydrous
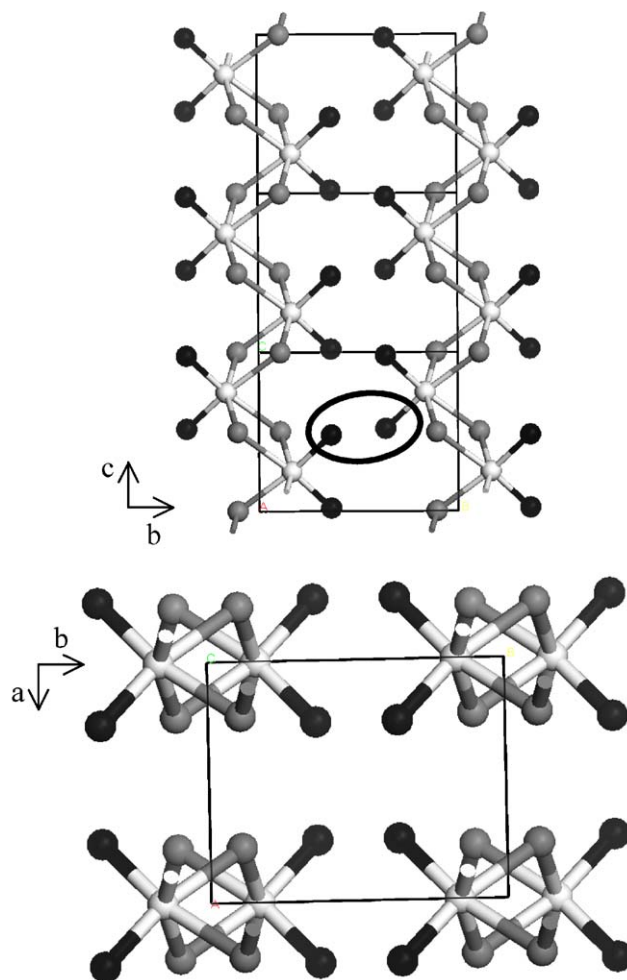

Fig. 7. $HfCl_4$ chain structure with substitution of mono-linked Cl atoms by OH (black balls), white ball = Hf and gray balls = bridged Cl atoms.

$HfCl_4$ at around $250\,^\circ C$, the low-temperature features are attributed to the decomposition of $HfOCl_2 \cdot nH_2O$ with $n \geqslant 4$ while the high-temperature ones ($T > 300\,^\circ C$) are due to the decomposition of $HfOCl_2 \cdot nH_2O$ with $n \leqslant 4$. The difference in thermal behavior between both sets of compounds is related to their structure, which is different depending on the hydration rate, leading to different structural evolution during heat-treatment with, before their transformation in hafnia, the formation of an hydroxide for $HfOCl_2 \cdot nH_2O$ with $n < 4$ and of an oxy-hydroxy-chloride for $n \geqslant 4$.

References

[1] U.A. Joshi, S.H. Chung, J.S. Lee, J. Solid State Chem. 178 (2005) 755–760.
[2] E. Barraud, Ph.D., INPL, Nancy, 2003.
[3] S. Bégin-Colin, G. Le Caër, E. Barraud, O. Humbert, J. Mater. Sci. 39 (2004) 5081–5089.
[4] E. Barraud, S. Bégin-Colin, G. Le Caër, J. Alloys Compd. 398 (2005) 208–218.
[5] A.M. Nartowski, I.P. Parkin, M. MacKenzie, A.J. Craven, I. MacLeod, J. Mater. Chem. 9 (1999) 1275–1281.

[6] A.L. Hector, I.P. Parkin, Polyhedron 14 (1995) 913–917.
[7] G. Shen, D. Chen, Y. Liu, K. Tang, Y. Qian, J. Cryst. Growth 262 (2004) 277–280.
[8] R. Tricot, Tech. Ing. 2360 (1994) 4–14.
[9] X. Feng, Y.-J. Bai, B. Lü, Y.-R. Zhao, J. Yang, J.-R. Chi, J. Cryst. Growth 262 (2004) 420–423.
[10] J. Fuller, M.D. Sacks (Guest Eds.), Special section on ultra-high, temperature ceramics (UHTC), J. Mater. Sci. 39 (2004) 5885–6066.
[11] L. Jeloaica, A. Estève, M. Djafari rouhani, D. Estève, Appl. Phys. Lett. 83 (2003) 542–544.
[12] L. Jeloaica, A. Estève, A. Dkhissi, D. Estève, M. Djafari rouhani, Comput. Mater. Sci. 33 (2005) 59–65.
[13] L. Kuklix, M. Ritala, T. Sajavaara, J. Keinonen, M. Leskela, Thin Solid Films 416 (2002) 72–79.
[14] K. Kaupo, J. Aarik, T. Uustare, J. Lu, M. Ritala, A. Aidla, L. Pung, A. Hårsta, M. Leskelä, A. Kikas, V. Sammelselg, Thin Solid Films 479 (2005) 1–11.
[15] S. Nonobe, N. Takahashi, T. Nakamura, Solid State Sci. 6 (2004) 1217–1219.
[16] J.H. Han, G. Guilian, Y. Widjaja, E. Garfunkel, C.B. Musgrave, Surf. Sci. 550 (2004) 199–212.
[17] E.P. Gusev, C. Cabral, M. Copel, C. D'Emic, M. Gribelyuk, Microelectron. Eng. 69 (2003) 145–151.
[18] A. Kytökivi, E.-L. Lakomaa, A. Root, H. Österholm, J.P. Jacobs, H.H. Brongersma, Langmuir 13 (1997) 2717–2725.
[19] M. Petersen, Comput. Mater. Sci. 30 (2004) 77–80.
[20] R. Tortevois, Ph.D., Université Paris VI, 1990.
[21] R.H. Nielsen, in: Ullmann's Encyclopedia of Industrial Chemistry, Wiley-VCH, Weinheim, 2002, pp. a28–543.
[22] R.H. Nielsen, in: Ullmann's Encyclopedia of Industrial Chemistry, Wiley-VCH, Weinheim, 2002, pp. a12–559.
[23] B. Beden, Ph.D.'s, Université de Poitiers, 1969, 1974.
[24] B. Beden, I. Guillaume, C. R. Acad. Sci. Sér. C 269 (1969) 1629–1632.
[25] B. Beden, I. Guillaume, C. R. Acad. Sci. Sér. C 270 (1970) 198–201.
[26] B. Beden, I. Guillaume, M.J. Martin, C. R. Acad. Sci. Sér. C 270 (1970) 34–36.
[27] A. Clearfield, P.A. Vaughan, Acta Cryst. 9 (1956) 555–558.
[28] A. Clearfield, Inorg. Chem. 3 (1964) 146–148.
[29] A. Clearfield, Rev. Pure Appl. Chem. 14 (1964) 91–108.
[30] A. Clearfield, J. Mater. Res. 5 (1990) 161–162.
[31] L.N. Komissarova, V.E. Plyushchev, I.N. Kremenskaya, Russ. J. Inorg. Chem. 5 (1960) 281–284.
[32] J.R. Fryer, J.L. Hutchinson, R. Paterson, Nature 226 (1970) 149–151.
[33] J.H. Canterford, R. Colton, Haildes of the Transitions Elements, Halides of the Second and Third Row Transition Metals, A Wiley Interscience Publication, Wiley, London, New York, Sydney, 1968.
[34] R. Srinivasan, C.R. Hubbard, O.B. Cavin, B.H. Davis, Chem. Mater. 5 (1993) 27–31.
[35] M. Li, Powder Technol. 137 (2003) 95–98.
[36] D.A. Powers, H.B. Gray, Inorg. Chem. 12 (1973) 2721–2726.
[37] A.F. Wells, Structural Inorganic Chemistry, fifth ed., Oxford University Press, Oxford, 1984.
[38] B. Krebs, Angew. Chem. Int. Ed. 8 (1969) 146–147.
[39] F.A. Cotton, G. Wilkinson, Advanced Inorganic Chemistry, fifth ed., A Wiley Interscience Publication, Wiley, London, New York, Sydney, 1988.
[40] A.F. Trotman-Dickenson (Ed.), Comprehensive Inorganic Chemistry, Pergamon Press, Oxford, 1973.
[41] G.Y. Guo, Y.L. Chen, W.J. Ying, Mater. Chem. Phys. 84 (2004) 308–314.
[42] J. Deabriges, Ph.D., Faculté des Sciences de Strasbourg, 1969.
[43] A. Benamira, Ph.D., Université Lyon I, 1997.
[44] B.M. Nirsha, B.V. Zhadanov, V.N. Malinovskii, N.N. Tyutyueva, N.E. Mtskhvetaridze, V.A. Olikova, Neorg. Mater. 22 (1986) 299–302.
[45] S. Takagi, J. Chem. Soc. Jpn. 75 (1954) 637–641.
[46] Physical constants of inorganic compounds, in: David R. Lide (Ed.), CRC Handbook of Chemistry and Physics, 78th ed., CRC Press, Boca Raton, FL, 1997, pp. 4–60.
[47] R.A. Nyquist, R.O. Kagel, Handbook of Infrared and Raman Spectra of Inorganic Compounds and Organic Salts, Infrared Spectra of Inorganic Compounds (3800–45 cm^{-1}), vol. 4, Academic Press, New York, 1971.
[48] G. Cerrato, S. Bordiga, S. Barbera, C. Morterra, Appl. Surf. Sci. 115 (1997) 53–65.
[49] T. Merle-Méjean, P. Barberis, S. Ben Othmane, F. Nardou, P.E. Quintard, J. Eur. Ceram. Soc. 18 (1998) 1579–2586.
[50] G.Y. Guo, Y.L. Chen, J. Solid State Chem. 178 (2005) 1675–1682.
[51] M. Pan, J.R. Liu, M.K. Lu, D. Xu, D.R. Yuan, D.R. Chen, P. Yang, Z.H. Yang, Thermochim. Acta 376 (2001) 77–82.